HHS Public Access

Author manuscript

Schizophr Res. Author manuscript; available in PMC 2022 February 01.

Published in final edited form as:

Schizophr Res. 2021 February ; 228: 60–73. doi:10.1016/j.schres.2020.12.016.

Abnormalities in the copper transporter CTR1 in postmortem hippocampus in schizophrenia: a subregion and laminar analysis.

Kirsten E. Schoonover[1], **Charlene B. Farmer**[2], **Charity J Morgan**[3], **Vidushi Sinha**[2], **Laura Odom**[2], **Rosalinda C. Roberts**[2]

[1]Department of Psychology and Behavioral Neuroscience, University of Alabama at Birmingham

[2]Department of Psychiatry and Behavioral Neurobiology, University of Alabama at Birmingham

[3]Department of Biostatistics, University of Alabama at Birmingham

Abstract

Dysbindin-1 modulates copper transport, which is crucial for cellular homeostasis. Several brain regions implicated in schizophrenia exhibit decreased levels of dysbindin-1, which may affect copper homeostasis therein. Our recent study showed decreased levels of dysbindin-1, the copper transporter-1 (CTR1) and copper in the substantia nigra in schizophrenia, providing the first evidence of disrupted copper transport in schizophrenia. In the present study, we hypothesized that there would be lower levels of dysbindin-1 and CTR1 in the hippocampus in schizophrenia versus a comparison group. Using semi-quantitative immunohistochemistry for dysbindin1 and CTR1, we measured the optical density in a layer specific fashion in the hippocampus and entorhinal cortex in ten subjects with schizophrenia and ten comparison subjects. Both regions were richly immunolabeled for CTR1 and dysbindin1 in both groups. In the superficial layers of the entorhinal cortex, CTR1 immunolabeled neuropil and cells showed lower optical density values in patients versus the comparison group. In the molecular layer of the dentate gyrus, patients had higher optical density values of CTR1 versus the comparison group. The density and distribution of dysbindin-1 immunolabeling was similar between groups. These laminar specific alterations of CTR1 in schizophrenia suggest abnormal copper transport in those locations.

Corresponding author information: Kirsten Schoonover, PhD, Department of Psychiatry, Translational Neuroscience Program, University of Pittsburgh, Phone: (304) 437-4554, schoonoverke@upmc.edu, Rosalinda C. Roberts, PhD, Department of Psychiatry and Behavioral Neurobiology, University of Alabama, Birmingham, Sparks Center 835C, 1720 2nd Ave South, Birmingham, AL 35233, Phone: 205-996-9373, rosalindaroberts@uabmc.edu.

Contributors

Dr. Roberts and Dr. Schoonover (while a graduate student in Dr. Roberts' lab) conceived of the experiments and wrote this paper together. Ms. Farmer and Dr. Schoonover performed the immunohistochemistry. Ms. Farmer photographed all of the areas for image analysis, analyzed all the data from one series of each antibody and supervised the undergraduates (VS and LO). Ms. Sinha analyzed one series of dysbindin immunolabeling. Dr. Schoonover and Ms. Odom analyzed one series of CTR1 immunolabeling. Dr. Morgan, a statistician, analyzed all of the data.

Conflict of interest

The authors have no conflicts of interest to declare.

Keywords

dysbindin; copper; DTNBP1 gene; immunohistochemistry; entorhinal cortex

1. Introduction

The dystrobrevin binding protein 1 (*DTNBP1*) gene codes for the dysbindin-1 protein family (Talbot et al., 2009). *DTNBP1* is expressed in regions of the brain that subserve cognitive function, such as prefrontal cortex and hippocampus (Weickert et al., 2004). *DTNBP1* modulates prefrontal function through an interaction with catachol o methyltransferase (COMT) (Papaleo et al., 2014). Allelic variations of *DTNBP1* have been associated with measures of executive function, cognitive ability, reward-based learning, and spatial, verbal, and working memory (Burdick et al., 2006; Wolf et al., 2011). *DTNBP1* allelic variations have been associated with impaired white matter integrity in healthy adults (Nickl-Jockschat et al., 2012), loss of gray matter volume in preteenagers (Tognin et al., 2011), and abnormalities in neurite outgrowth and morphology (Dickman and Davis, 2009). Dysbindin has an important role in calcium-dependent vesicle release at glutamatergic synapses (Dickman and Davis, 2009). Dysbindin is a subunit of the BLOC-1 complex (biogenesis of lysosome-related organelles complex 1) and is involved in synaptic vesicle trafficking, neurite outgrowth and development, synaptic plasticity, and lysosomal homeostasis (Nazarian et al., 2006; Ghiani et al., 2010; Mullin et al., 2015).

DTNBP1 is considered by many (Bray et al., 2005; Marshall et al., 2017; Norton et al., 2006; Pae et al., 2008; Riley et al., 2009; Straub et al., 2002; Voisey et al., 2010; Zatz et al., 1993), but not all (Farrell et al., 2015; Mutsuddi et al., 2006; Schizophrenia Working Group, 2014) to be a susceptibility gene for schizophrenia. *DTNBP1* allelic variability is associated with cognitive abnormalities in patients with first-episode psychosis (Varela-Gomez et al., 2015), and influences the severity of cognitive decline in schizophrenia (Burdick et al., 2007). Genetic variations that reduce dysbindin-1 expression can identify in which subjects (both humans and mice) antipsychotic drugs will likely improve cognitive impairments (Scheggia et al., 2018). Furthermore, decreases in dysbindin-1 protein and gene expression have been observed in postmortem cortex, midbrain, and hippocampus in patients with schizophrenia (Tang et al., 2009; Talbot et al., 2004, 2009, 2011; Weickert et al., 2004, 2008). In our recent study, we found lower protein levels of the B/C isoforms of dysbindin-1 in the substantia nigra of patients with schizophrenia compared to controls (Schoonover et al., 2018). Together, these data suggest that dysbindin may play a role in the psychopathology and neuropathology in schizophrenia.

Interestingly, knockout of *DTNBP1* in animal models decreases the copper transporters ATP7A and copper transporter-1 (CTR1) (Gokhale et al., 2015). Copper is required for normal development and homeostatic function due to its crucial role for many cellular functions such as monoamine metabolism, mitochondrial activity, and myelination (Scheiber et al., 2010). Copper is transported from the bloodstream across the blood brain barrier (Eisses and Kaplan, 2005). Endothelial cells at the blood brain barrier take up copper from the blood via CTR1, and release copper into the brain parenchyma via ATP7A (Scheiber et

al., 2010). Copper then is transported into astrocytes and then neurons via CTR1 (Scheiber et al., 2010). Once inside the cell, copper is bound by metallochaperones and delivered to the trans-Golgi network (Maryon et al., 2013). ATP7A is located within the trans-Golgi network (Petris et al., 1996; Yamaguchi et al., 1996) and distributes copper to metallochaperones (e.g., SCO1) which transport copper to the needed location within the cell (Davies et al., 2013; Leary et al., 2007). Copper is differentially distributed across brain regions (Davies et al., 2013) and is found in region specific intracellular locations (Sato et al., 1994). Dysfunctional peripheral copper absorption or secretion results in Wilson's or Menkes disease, characterized by copper toxicity or deficiency, respectively (Menkes et al., 1962; Wilson, 1934). CTR1 knockdown and/or loss results in developmental defects and lethality (Lee et al., 2001), and total loss of ATP7A results in Menkes disease and lethality (Menkes et al., 1962), exemplifying the incredible importance of these transporters in normal homeostasis and function.

In animal models, decreased copper produces demyelination and decreased oligodendrocytic protein expression (Herring and Konradi, 2011; Matsushima and Morell, 2001). Rats fed the copper chelating agent cuprizone showed regionally specific decreased expression of mRNA transcripts encoding oligodendrocytic proteins. Importantly, copper deficits produce schizophrenia-like behavioral impairments, such as deficits in novel object recognition, working memory, spatial memory, pre-pulse inhibition, social interaction and anxiety (Gregg et al., 2009; Herring and Konradi, 2011; Talbot, 2009). Behavioral deficits and pathology can be reversed with antipsychotic treatment (Xuan et al., 2015; Zhang et al., 2008). Apart from our recent work suggesting a deficit in copper transport and showing a deficit in copper content in the substantia nigra in schizophrenia (Schoonover et al., 2018), the role of copper in schizophrenia has been limited to measurements of copper content in peripheral blood (Vidovic et al., 2013, and references therein).

Candidate gene studies suggest that there are abnormalities in dysbindini-1 in schizophrenia. Dysbindin knockout mice show decreases in copper transporters (Gokhale et al., 2015). Copper levels are increased in the blood of patients of schizophrenia (Vidovic et al., 2013), but are decreased in the brain parenchyma along with dysbindin and copper transporters (Schoonover et al., 2018), suggesting abnormal transport of copper across the blood brain barrier. The hippocampus is abnormal in schizophrenia, including decreases in mRNA levels of *DTNBP1* (Weickert et al., 2008). Therefore, we hypothesized schizophrenia patients would exhibit deficits in dysbindin-1 and copper transport, as measured by the copper transporter CTR1, within the hippocampus. We chose not to measure ATP7A or ATP7B because in our recent study of the substantia nigra, there were no changes in APT7B and only changes in ATP7A in off drug patients. Moreover, there were no changes in ATP7A in the cingulum bundle or the cortex in either on or off drug patients (unpublished data). Thus, using semi-quantitative immunohistochemistry, we measured dysbindin-1 and the copper transporter CTR1, in postmortem hippocampus from schizophrenia patients and a matched comparison group. This work has been presented in preliminary form (Roberts et al., 2019).

2. Methods

2.1 Postmortem Brains

In this study, we used immunohistochemistry to localize CTR1 and dysbindin-1 in the hippocampus of 10 schizophrenia cases and 10 comparison cases. Tissue was obtained from the Maryland Brain Collection and the Alabama Brain Collection, and was collected in compliance with IRB-approved protocols and in accordance with all relevant guidelines and procedures. The work completed in this study was approved by the IRB (F080306003) at the University of Alabama at Birmingham. Cases were diagnosed and assessed based on information obtained from medical records and phone interviews with next of kin. Informed consent was obtained for the use of brain tissue, phone interview, and for access to medical records for research purposes. Tissue was obtained and used in a manner compliant with the Declaration of Helsinki. Exclusionary criteria for this cohort were history/evidence of intravenous drug abuse, HIV/AIDS, hepatitis B, head trauma, comorbid neurological disorders, custodial death, fire victims, unknown next of kin, children or decomposed subjects. Two psychiatrists established the DSM diagnoses (DSM-III-R through DSM-IV-TR) using the current Structured Clinical Interview for the DSM at the time of diagnosis. Clinical information was obtained from autopsy and medical records, in addition to family interviews. Comparison brains had sufficient information to verify a lack of major psychiatric (other than alcoholism) or neurological disease.

Demographic information is listed in Table 1. The mean age, pH, and time in fixative were similar between groups. Both groups had a similar gender and racial composition. The only statistically significant difference between groups was between the mean post-mortem intervals, which were 6.7±1.42 hours in the comparison group vs. 5.2±1.55 hours in the patient group, which may not be biologically significant.

2.2 Tissue Preparation and Antibody Validation

The hippocampi were immersed in cold 4% paraformaldehyde and 1% glutaraldehyde in 0.1 M phosphate buffer (PB), pH 7.4. The tissue was stored in this fixative at 4°C until it was further subdissected (Figure 1A). The anterior body of the hippocampus was then sectioned with a vibratome (Leica MICROM HM 650V) into six series of 40-μm thick sections. Sections from two adjacent series were prepared for the immunohistochemical localization of CTR1 using polyclonal rabbit anti-CTR1 (Novus Biologicals NB100–402) or dysbindin using monoclonal rabbit anti-dysbindin (Abcam ab133652). Antibody concentrations were initially optimized in a dilution series. Antibody controls consisted of omission of the primary antibody and/or blocking peptides raised to CTR1, both of which resulted in no immunolabeling (Figures 3B, 4,C,D, 7B,C). In a separate publication, we previously verified the specificity of the dysbindin antibody in western blot studies with preadsorption and by absent band density in the dysbindin knock out mice (Schoonover et al., 2018). Knockout of CTR1 is embryonic lethal (Lee et al., 2001), so we were not able to test the antibody using these mice.

2.3 Immunohistochemistry

For each antibody, tissue from all subjects was processed in five batches within 10 days of one another. Free-floating sections from two patients and two cases from the comparison group were immunostained in each run, with eight sections per case per antibody, with sections separated by at least 240 μm. Sections were incubated for 15 minutes at room temperature (RT) in a solution of 1% sodium borohydride in 0.01M phosphate buffered saline (PBS) while agitating. After that, sections were incubated in a solution of 5% hydrogen peroxide in 0.01M PBS for 30 minutes at RT while agitating. Then, sections were incubated in a solution of 10% normal goat serum in 0.01 M PBS for one hour at RT while being agitated.

The sections were then incubated for 48 hours at 4°C in their respective antibody solutions of 3% normal goat serum in 0.01 M PBS: polyclonal rabbit anti-CTR1 antibody (Novus Biologicals NB100–402) at a dilution of 1:4000 and monoclonal rabbit anti-dysbindin1 (Abcam ab133652) at a dilution of 1:1000. Sections were incubated for 45 minutes while being agitated at RT in a solution of biotinylated anti-rabbit secondary antibody at a dilution of 1:267 and 3% normal goat serum in 0.01 M PBS. The sections were then incubated in avidin-biotin complex (1:100 dilution) for 45 minutes while agitated at RT. To visualize the reaction product, sections were incubated for 4 minutes in a 3, 3’-diaminobenzidine solution (10 mg diaminobenzidine, 15 ml PBS, 12μL 0.03% hydrogen peroxide; Vector Laboratories, SK-4100).

All sections from each case were mounted on charged slides, and dried at RT overnight. A Nissl stain procedure was used to counterstain one section from each series. All slides were placed in increasing concentrations of ethanol and then in xylene for dehydration. Eukitt was used to coverslip the slides.

2.4 Microscopy

A Nikon DS-Fi1 color digital camera connected to a Nikon Eclipse 50i microscope was used to take photomicrographs of the sections. Specific regions that were photographed are shown in diagram form (Figure 1B) and in a tissue section immunolabeled with dysbindin (Figure 1C). All photomicrographs of CTR1 immunolabeled sections were taken at the same microscope and camera settings: with a 20X lens, aperture of 0.4, quality capture (2560×1920 pixels), exposure length of six milliseconds, medium contrast, and a gain of 1.2. All photomicrographs of dysbindin immunolabeled sections were taken at the same microscope and camera settings: with a 20X lens, aperture of 0.75, quality capture (2560×1920 pixels), exposure length of 15 milliseconds, medium contrast, and a gain of 1.2. Each photomicrograph was 0.283mm^2, yielding a total of 1.698mm^2 analyzed per area (6 micrographs X 0.283mm^2).

All photomicrographs were taken by author CBF from the following 19 areas: entorhinal cortex (superficial layers, pyramidal cell layer, subcortical white matter), subiculum (superficial layers, pyramidal cell layer, subcortical white matter), CA1 (stratum oriens, pyramidale, radiatum, and lacunosum/ moleculare), CA3 (stratum oriens, pyramidale, and radiatum/ lacunosum/ moleculare), dentate gyrus (granule cell layer, molecular layer and

polymorphic layer), the alveus over CA1 and over CA3, and the fornix. Superficial layers of the subiculum and entorhinal cortex refer to the distal, apical dendritic region (Figure 1B). Two series of sections, yielding a total of six sections, were analyzed for each marker. Photomicrographs were taken from all six sections for each antibody for each case (not including Nissl counterstain), with three micrographs of each layer of each region taken for a total of 57 pictures taken per tissue section.

2.5 Data Collection

The density of immunohistochemical labeling was assessed using optical densitometry as previously described (Mabry et al., 2019; McCollum et al., 2016). The photographs were opened in Adobe Photoshop for data collection. Photomicrographs were inverted and then the layer/region of interest was selected using the lasso, marquee or quick select tool. Optical density measurements were recorded separately for immunolabeling in gray matter for the whole region, cell immunolabeling, and neuropil immunolabeling. Optical density measurements were recorded separately for immunolabeling in white matter for the whole region, glial immunolabeling, and fiber immunolabeling. To select the whole region of interest, a box tool was selected. Artifacts on the slide such as bubbles, folds in the tissue or the occasional piece of debris were avoided during photography and data collection. Immunolabeled cells were measured using the quick selection tool. Neuropil or white matter areas were measured using the magic wand tool. This tool is ideal for measuring irregularly shaped tissue between the neurons or glia. The gray mean value was recorded for the slide itself (where no tissue was located) and used for background subtraction.

2.6 Statistics

Two complete series of sections were analyzed for each marker and combined for statistical analysis. All analyses were conducted using SAS version 9.4 (Cary, NC). For each measure (CTR1 or Dys) and region, means and standard errors (SE) were calculated for each group. Unpaired t-tests were used to test for group differences in demographics and tissue quality. A chi-square test was used for categorical variables (sex, race). Linear mixed models were used to test for group differences after controlling for race, sex, age of subject, and the person analyzing the data (KES,CBF, LO, VS); these models included a random effect for subject in order to control for potential correlation among sections within a subject. Visual inspection of plots of the model residuals was used to check for departures from normality.

3. Results

3.1 CTR1

3.1.1 Description of CTR1 immunolabeling—The hippocampus proper and dentate gyrus were richly immunolabeled for CTR1 in both the comparison group and schizophrenia patients (Figure 1D,E). CTR1 immunolabeled the hippocampus in a characteristic pattern dependent on the layer. Qualitatively, CTR1 immunolabeling was present in the same cell types in both groups. In both the comparison group and the patients, immunolabeling was more prominent in the DG, the pyramidal layers of CA1-CA3 and the gray matter in the subiculum and entorhinal cortex than other areas. There was less immunolabeling in white

matter structures (alveus, fornix), and the molecular layer of CA1-CA3 leading to noticeable demarcations between adjacent layers.

The somata and apical dendrites of pyramidal neurons were robustly immunolabeled in entorhinal cortex (Figure 2A), CA3 (Figure 2B), CA1 (Figure 2C) and the subiculum (Figure 2D). In stratum oriens and stratum lacunosum, immunolabeled fibers were present (Figure 2B). Immunolabeling was present throughout the dentate gyrus (Figure 3). The polymorphic layer contained lightly immunolabeled neurons and fibers (Figure 3A). It was often difficult to determine whether immunolabeling in the granule cell layer was in granule cells or in the surrounding neuropil (Figure 3A). However, individual immunolabeled granule cells and interneurons could be distinguished from the neuropil in fortuitous sections (Figure 3C). Labelled endothelial processes were identified (Figure 2D).

Immunolabeling of the white matter of the hippocampus revealed immunolabeled glial cells, fibers and punctate structures (Figure 4). The fornix (Figure 4A,C), entorhinal cortex (Figure 4E) and alveus (Figure 4D) were all labeled in a similar way. However, labeled punctate structures were especially prominent in the fornix and were determined to be the bulbous portions of fibrous astrocytes in a preliminary electron microscopic study (Nguyen et al. 2017). Labelled endothelial cells were identified in (Figure 4A,C,E).

3.1.2 Quantitative analysis—

CTR1 immunolabeling was quantified throughout each cellular domain of the hippocampus in the comparison group and patients with schizophrenia (Supplementary Table 1). Only CTR1 immunolabeling in the entorhinal cortex and dentate gyrus showed significant differences between groups (Figures 5, 6). In the superficial area of the entorhinal cortex, both fibers (neuropil) and cells showed lower optical density values in the schizophrenia patients than in the comparison group (Figures 5A,B, 6). Both cells and the entire image of the molecular layer in the dentate gyrus had significantly higher optical density values in schizophrenia patients than in the comparison group (Figures 5C,D, 6).

3.2 Dysbindin

3.2.1 Description of dysbindin immunolabeling—

The hippocampus proper and dentate gyrus were richly immunolabeled for dysbindin in both the comparison group and schizophrenia patients (Figure 7A). Qualitatively, dysbindin immunolabeling was more robust in the gray matter vs. white matter. Immunolabeling was present throughout the pyramidal layers of CA1 and CA3, and within the gray matter of the subiculum and entorhinal cortex (Figure 8). The somata and apical dendrites of pyramidal neurons were robustly immunolabeled in entorhinal cortex (Figure 8A), CA3 (Figure 8B), CA1 (Figure 8C) and the subiculum (Figure 8D). Neurons were immunolabeled in the polymorphic layer of the dentate gyrus (Figure 9A). Dense immunolabeling was present in the granule cell (Figure 9A–C), but it was often impossible to distinguish cell body labeling from neuropil labeling.

Dysbindin immunolabeling in white matter was not as robust as in the gray matter. Compared to cellular layers, decreased levels of immunolabeling were observed in the alveus and fornix, as well as the molecular layer of CA1 - CA3. Immunolabeled glial cells,

endothelial cells, fibers and punctate structures were observed (Figure 10). This pattern of immunolabeling was very similar to that of CTR1, resulting in noticeable layer demarcation.

3.2.2 Quantitative analysis—Dysbindin immunolabeling was quantified throughout each cellular domain of the hippocampus in comparison subjects and patients with schizophrenia (Supplementary Table 2). The density and distribution of dysbindin immunolabeling was similar between groups with no significant differences.

4. Discussion

In the present study, we described and quantified CTR1 and dysbindin immunolabeling in the hippocampus of patients with schizophrenia and a comparison group. To our knowledge, this is the first report of CTR1 localization in the human hippocampus other than our preliminary report (Nguyen et al., 2017). In the current study, we found that the density of CTR1 labeling was decreased in the superficial layers of the entorhinal cortex, where apical dendrites of pyramidal cells reside, in schizophrenia subjects when compared to the comparison group. Specifically, cells and fibers of these outer layers exhibited less intense immunolabeling. In contrast, the molecular layer of the dentate gyrus exhibited more CTR1 labeling in patients with schizophrenia. No statistically significant alterations in dysbindin-1 immunostaining were observed.

4.1 Limitations

The current study possesses some limitations. Due to the nature of postmortem studies, our analysis only captures a picture of CTR1 and dysbindin-1 immunolabeling at the time of death; however, by matching for postmortem interval and pH and excluding causes of death known to affect agonal status (Stan et al., 2006) we can presume the results shown here are not postmortem artifact. As is typical for postmortem studies, the schizophrenia subjects had been treated with various antipsychotic drugs prior to death and were not first-episode, or antipsychotic drug naïve. While no effect of antipsychotics on CTR1 or dysbindin-1 was observed via Western blot in the substantia nigra (Schoonover et al., 2018), it is of course possible that the impact of treatment on these markers is brain region-specific. In addition, severity and heterogeneity of symptoms, as well as varying treatment response can also confound results; that said postmortem studies are very valuable and add to gaps in the literature that no other technique can provide (McCullumsmith et al., 2014). Immunohistochemistry is considered by some to be semi-quantitative technique. Thus, we made every effort to match the samples according to fixation time, and we processed patients and comparison subjects in the same run. In addition, two or more individuals measured optical density and the data were merged for statistical analysis. That said one must interpret these findings with a certain degree of caution. We were unable to assess layer-specific measurements of cellular copper content to correlate with the markers measured here, and therefore the impact of the observed alterations on cellular copper levels within the hippocampus remains unknown. It must be acknowledged that many things can effect copper levels including diet (Morrell et al., 2017), smoking (Badea et al., 2018), and alcohol (Grochowski et al., 2019), parameters that we could not control or eliminate due to wide spread variability and use in patients with schizophrenia.

4.2 CTR1

CTR1 was found in neuronal populations as seen previously in neurons of the dorsal root ganglion (Ip et al., 2010). Based on morphology and layer specific location, CTR1 was localized mainly, but not exclusively, in excitatory neurons in both groups, consistent with the role of copper in excitatory neurotransmission (Hartter and Barnea, 1988; Hopt et al., 2003; Kardos et al., 1989; Marchetti, 2014). Immunolabeling was also prominent in white matter structures. The entorhinal cortex is the beginning point of the trisynaptic pathway (Figure 1B). This region receives projections from several cortical areas that converge on the apical dendrites of pyramidal cells, what we refer to as the superficial layers (Mohedano-Moriano et al., 2007). Our finding of decreased CTR1 immunolabeling in the superficial layers of the entorhinal cortex in schizophrenia subjects compared to the comparison group suggests a deficit of copper signaling in this area, which could impact signaling throughout the trisynaptic pathway. Given that copper is neurotoxic in excess quantities, downregulated CTR1 could be a compensatory mechanism to protect the cells from excess extracellular copper and cuprinergic signaling. However, such a compensation is unlikely to be occurring here. Previous work by our group revealed a decrease of CTR1 and a decrease of cellular copper content in the postmortem substantia nigra of subjects with schizophrenia (Schoonover et al., 2018). These data, taken in conjunction with the excess of plasma copper content in schizophrenia (Vidovic et al., 2013, and references therein), suggest that the downregulation of CTR1 observed in the entorhinal cortex in the current study is not stemming from excess cuprinergic signaling. Furthermore, literature assessing the activity of regions projecting to the entorhinal cortex in schizophrenia indicate an overall downregulation of activity (Ikuta et al., 2012), providing additional evidence that the decrease of CTR1 observed here is not resulting from stimulation excess.

Additionally, our finding of decreased CTR1 immunolabeling within neurons and fibers in the superficial layers of the entorhinal cortex suggests that deficient copper in schizophrenia may be a mechanism to downregulate hippocampal activity. Copper is intrinsically involved in ATP synthesis and excitatory signaling. Copper is delivered by the metallochaperone, SCO1, to the catalytic core of cytochrome C oxidase required for ATP synthesis (Leary et al., 2007). Without copper, ATP synthesis is downregulated and the overall energy metabolism of the region is decreased. Additionally, copper is implicit in neuronal signaling and synaptic function. Copper is released from neurons during depolarization and can modulate both GABA- and glutamatergic receptors (Hartter and Barnea, 1988; Hopt et al., 2003; Kardos et al., 1989; Marchetti, 2014). Therefore, our findings of decreased CTR1 immunolabeling in both cells and fibers of the superficial layers of the entorhinal cortex suggest an overall downregulation of cuprinergic signaling that could have widespread pathological effects.

Our finding of decreased CTR1 in the cells and fibers of the superficial layers of the entorhinal cortex lends is consistent with the importance of copper in myelin integrity and dendritic spine formation, as well as cellular function. Deficits of myelin and associated oligodendrocytes have been well replicated in schizophrenia in several brain regions (Samartzis et al., 2014; Seitz et al., 2016). Cortical areas exhibit decreased markers of myelin basic protein (a key component of myelin), fewer oligodendrocytes, abnormal

oligodendrocyte morphology, oligodendrocyte degeneration, myelin thickness and laminar abnormalities, as well as downregulation of key myelin related genes and proteins in schizophrenia (Buchsbaum et al., 1998; Chambers et al., 2004; Hakak et al., 2001; Hof et al., 2002; Lim et al., 1999; Schoonover et al., 2019; Sigmundsson et al., 2001; Uranova et al., 2007; Vostrikov et al., 2008). Interestingly, application of the copper chelator cuprizone results in massive, albeit reversible, demyelination and oligodendrocyte death (Xuan et al., 2015; Zhang et al., 2008), indicating that copper must play a crucial role in myelin and oligodendrocyte function and integrity. If a deficit of cuprinergic signaling and copper content exists in the superficial layers of the entorhinal cortex in schizophrenia as indicated by our finding of decreased CTR1, this could impact white matter integrity in this area.

In contrast to our findings in the superficial layers of the entorhinal cortex, we observed significantly elevated immunolabeling of CTR1 in the molecular layer of the dentate gyrus, consistent with a trending increase of CTR1 mRNA within the middle temporal area (Roussos et al., 2012) as revealed via Kaleidoscope genetic database (Alganem et al., 2020). The molecular layer of the dentate gyrus is a relatively neuron-free layer and comprised of the dendrites of the granule cells (Amaral et al., 2007). Therefore, cell labeling in this area is due to glial cells and immunolabeling in the whole region combined largely reflects neuropil. Given the deficit of CTR1 immunolabeling in the superficial entorhinal cortex observed here, and that the entorhinal cortex projects to the dentate gyrus in the trisynaptic pathway of the hippocampus, perhaps such an upregulation of CTR1 in the dentate gyrus is a compensatory effect. The dentate gyrus exhibits an incredible cellular need for copper, as demonstrated by high levels of copper superoxide dismutase (Liu et al., 1993) and that copper deficiency during development results in abnormal maturation of the dentate gyrus and hippocampus proper (Hunt and Idso, 1995). Therefore, given the need of copper (and hence CTR1) by dendrites and their spines (Perrin et al., 2017), it would be logical to regard such an increase as a compensatory reaction to a lack of copper within the hippocampus-similar to upregulation of neurotransmitter receptors after application of the relevant antagonist (Follesa et al., 1996).

In further support of our suggestion of compensatory upregulation of CTR1 in the molecular layer of the dentate gyrus in response to copper deficit is the observation that the dentate gyrus exhibits deficient signaling in schizophrenia (Stan et al., 2015). Decreased glutamatergic signaling has been observed in schizophrenia dentate gyrus, which has been associated with a decrease of excitatory receptors within the region (Stan et al., 2015). Furthermore, the dentate gyrus exhibits downregulation of energy metabolism genes in schizophrenia such as cytochrome c oxidase. Therefore, downregulated activity of the dentate gyrus and our finding of potentially compensatory elevated CTR1 in the molecular layer together is consistent with copper playing a key role in neuronal activity and the dysregulations observed in schizophrenia.

4.3 Dysbindin

Surprisingly, we did not observe any alterations of dysbindin-1 in the hippocampus in our schizophrenia cohort. Previous literature suggested downregulation of both dysbindin1 mRNA and protein in the hippocampus in schizophrenia (Talbot et al., 2011; Tang et al.,

2009; Weickert et al., 2004, 2008). However, these differences have been isoform, laminar, and study specific. Decreased mRNA has been found in the polymorphic layer and inner molecular layer of the DG, the subiculum, CA1, and the stratum oriens and radiatum of CA3 (Weickert et al., 2008), though analysis of *DTNBP1* mRNA within the broader middle temporal area (Roussos et al., 2012) was consistent with our results as revealed by the Kaleidoscope genetic database (Alganem et al., 2020). Dysbindin-1 has three isoforms known as dysbindin 1A, 1B, and 1C (Talbot et al., 2009, 2011). Dysbindin 1A is found in the post-synaptic density and thought to be involved in dendritic spine homeostasis, while dysbindin 1B is found exclusively in synaptic vesicles in the presynaptic axon terminal (Talbot et al., 2011), and is involved in glutamatergic transmission (Numakawa et al., 2004). Dysbindin 1C is found in both places, but primarily is located in the post-synaptic density and involved in dendritic spine function (Talbot et al., 2011). Most, but not all, studies have shown decreases in specific dysbindin isoforms in schizophrenia patients (Schoonover et al., 2018; Talbot et al., 2004; Tang et al., 2009; Weickert et al., 2004, 2008). Decreased protein levels of isoforms 1B and 1C have been observed in the hippocampus (Talbot et al., 2011) whereas we dysbindin 1C levels were lower in the dorsolateral prefrontal cortex of schizophrenia subjects (Tang et al., 2009). Indeed, our previous work observed that schizophrenia patients had decreased protein levels of dysbindin 1B/C, but not isoform 1A in postmortem substantia nigra (Schoonover et al., 2018). Perhaps no differences of dysbindin-1 were observed in the current study because of isoform-specific alterations, or methodological differences. For instance, changes in mRNA do not always indicate protein changes. Moreover, western blot analysis of the whole hippocampus was used in the study by Talbot et al., (2011), making it difficult to compare their results to individual layer specific quantification performed in the present study. Finally, the antibody used in the present study labels all three isoforms (Schoonover et al., 2018), and perhaps a deficit in one isoform was cancelled out by no alterations in another. Further work to assess specific isoforms of dysbindin-1 in the schizophrenia hippocampus would ameliorate this issue.

4.4 Summary

Taken together, our data suggest dysregulation of copper transport and homeostasis in the hippocampus and entorhinal cortex in schizophrenia that is region and layer specific, a potential mechanism of schizophrenia pathology that was previously unstudied. Deficient copper within the hippocampus could have deleterious effects, including decreased energy metabolism and neuronal signaling, deficits of myelin maintenance and integrity, and an overall pathological modulation of the trisynaptic pathway crucially involved in memory and cortical function (Gregg et al., 2009; Herring and Konradi, 2011; Talbot, 2009). Therefore, further study is needed to assess cellular copper content and transporter status of each layer and cell type of the hippocampus in schizophrenia, as well as replication of the current study. Abnormal copper and other trace metals are becoming increasingly associated with schizophrenia and other forms of psychosis (Bitanihirwe and Cunningham, 2009; Joe et al., 2018; Schoonover et al., 2018) and therefore could provide a new mechanism to be targeted for development of better treatments. For instance, treatments that mimic the functions of CTR1 might enhance copper transport from the blood to the brain parenchyma could be therapeutic.

Supplementary Material

Refer to Web version on PubMed Central for supplementary material.

Acknowledgments

We would like to thank the staff of the Maryland and Alabama Brain Collections and the donors and their families for the brain donations.

Role of funding sources

This research was supported by NINDS F99NS105208 (KES), NIMH R21MH108867 (RCR) and NIMH R21117434 (RCR). The funding sources paid for salary, supplies, and travel to meetings. The funding sources had no role in study design, data collection, analysis and interpretation of data, writing the manuscript, or in the decision to submit the paper for publication.

8. References

Amaral DG, Scharfman HE, Lavenex P, 2007. The dentate gyrus: fundamental neuroanatomical organization (dentate gyrus for dummies). Prog Brain Res.163:3–22. [PubMed: 17765709]

Signature. bioRxiv 2020.05.01.070805; doi: 10.1101/2020.05.01.070805

Alganem K, Shukla R, Eby H, Abel M, Zhang X, McIntyre WB, Lee J, Au-Yeung C, Asgariroozbehani R, Panda R, O'Donovan SM, Funk A, Hahn M, Meller J, McCullumsmith R, 2020. Kaleidoscope: A new bioinformatics pipeline web application for in silico hypothesis exploration of omics signature. bioRxiv 05.01.070805; doi: 10.1101/2020.05.01.070805

Badea M, Luzardo OP, González-Antuña A, Zumbado M, Rogozea L, Floroian L, Alexandrescu D, Moga M, Gaman L, Radoi M, Boada LD, Henríquez-Hernández LA, 2018. Body burden of toxic metals and rare earth elements in non-smokers, cigarette smokers and electronic cigarette users. Environ Res. 166:269–275. [PubMed: 29908458]

Bitanihirwe BK, Cunningham MG, 2009. Zinc: the brain's dark horse. Synapse 63(11):1029–49. [PubMed: 19623531]

Bray NJ, Preece A, Williams NM, Moskvina V, Buckland PR, Owen MJ, O'Donovan MC, 2005. Haplotypes at the dystrobrevin binding protein 1 (DTNBP1) gene locus mediate risk for schizophrenia through reduced DTNBP1 expression. Hum Mol Genet. 14(14):1947–54. [PubMed: 15917270]

Buchsbaum MS, Tang CY, Peled S, Gudbjartsson H, Lu D, Hazlett EA, Downhill J, Haznedar M, Fallon JH, Atlas SW, 1998. MRI white matter diffusion anisotropy and PET metabolic rate in schizophrenia. Neuroreport 9(3):425–30. [PubMed: 9512384]

Burdick KE, Goldberg TE, Funke B, Bates JA, Lencz T, Kucherlapati R, Malhotra AK, 2007. DTNBP1 genotype influences cognitive decline in schizophrenia. Schizophr Res. 89(1–3):169–72. [PubMed: 17074466]

Burdick KE, Lencz T, Funke B, Finn CT, Szeszko PR, Kane JM, Kucherlapati R, Malhotra AK, 2006. Genetic variation in DTNBP1 influences general cognitive ability. Hum Mol Genet. 15(10):1563–8. [PubMed: 16415041]

Chambers JS, Perrone-Bizzozero NI, 2004. Altered myelination of the hippocampal formation in subjects with schizophrenia and bipolar disorder. Neurochem Res. 29(12):2293–302. [PubMed: 15672553]

Davies KM, Hare DJ, Cottam V, Chen N, Hilgers L, Halliday G, Mercer JF, Double KL, 2013. Localization of copper and copper transporters in the human brain. Metallomics 5(1):43–51. [PubMed: 23076575]

Dickman DK, Davis GW, 2009. The schizophrenia susceptibility gene dysbindin controls synaptic homeostasis. Science 326: 1127–1130. [PubMed: 19965435]

Eisses JF, Kaplan JH, 2005. The mechanism of copper uptake mediated by human CTR1: a mutational analysis. J Biol Chem. 280:37159–37168. [PubMed: 16135512]

Farrell MS, Werge T, Sklar P, Owen MJ, Ophoff RA, O'Donovan MC, Corvin A, Cichon S, Sullivan PF, 2015. Evaluating historical candidate genes for schizophrenia. Mol Psych. 20(5):555–62.

Follesa P, Ticku MK, 1996. NMDA receptor upregulation: molecular studies in cultured mouse cortical neurons after chronic antagonist exposure. J Neurosci.16(7):2172–8. [PubMed: 8601798]

Ghiani CA, Starcevic M, Rodriguez-Fernandez IA, Nazarian R, Cheli VT, Chan LN, Malvar JS, de Vellis J, Sabatti C, Dell'Angelica EC, 2010. The dysbindin-containing complex (BLOC-1) in brain: developmental regulation, interaction with SNARE proteins and role in neurite outgrowth. Mol. Psych 15, 204–215.

Gokhale A, Vrailas-Mortimer A, Larimore J, Comstra HS, Zlatic SA, Werner E, Manvich DF, Iuvone PM, Weinshenker D, Faundez V, 2015. Neuronal copper homeostasis susceptibility by genetic defects in dysbindin, a schizophrenia susceptibility factor. Hum Mol Genet. 24(19):5512–23. [PubMed: 26199316]

Gregg JR, Herring NR, Naydenov AV, Hanlin RP, Konradi C, 2009. Downregulation of oligodendrocyte transcripts is associated with impaired prefrontal cortex function in rats. Schizophr Res.113(2–3):277–87. [PubMed: 19570651]

Grochowski C, Blicharska E, Baj J, Mierzwińska A, Brzozowska K, Forma A, Maciejewski R 2019. Serum iron, Magnesium, Copper, and Manganese Levels in Alcoholism: A Systematic Review. Molecules. 2019 4 7;24(7).

Hakak Y, Walker JR, Li C, Wong WH, Davis KL, Buxbaum JD, Haroutunian V, Fienberg AA, 2001. Genome-wide expression analysis reveals dysregulation of myelination-related genes in chronic schizophrenia. Proc Natl Acad Sci USA. 98(8):4746–51. [PubMed: 11296301]

Hartter DE, Barnea A,1988. Evidence for release of copper in the brain: depolarization-induced release of newly taken-up 67copper. Synapse 2(4):412–5. [PubMed: 3187909]

Herring NR, Konradi C, 2011. Myelin, copper, and the cuprizone model of schizophrenia. Front Biosci (Schol Ed) 3(3):23–40. [PubMed: 21196354]

Hof PR, Haroutunian V, Copland C, Davis KL, Buxbaum JD, 2002. Molecular and cellular evidence for an oligodendrocyte abnormality in schizophrenia. Neurochem Res. 27(10):1193–200. [PubMed: 12462417]

Hopt A, Korte S, Fink H, Panne U, Niessner R, Jahn R, Kretzschmar H, Herms J, 2003. Methods for studying synaptosomal copper release. J Neurosci Methods 128(1–2):159–72. [PubMed: 12948559]

Hunt CD, Idso JP, 1995. Moderate copper deprivation during gestation and lactation affects dentate gyrus and hippocampal maturation in immature male rats. J Nutr. 125(10):2700–10. [PubMed: 7562107]

Ikuta T, Szeszko PR, Gruner P, DeRosse P, Gallego J, Malhotra AK, 2012. Abnormal anterior cingulate cortex activity predicts functional disability in schizophrenia. Schizophr Res.137(1–3):267–8. [PubMed: 22406209]

Ip V, Liu JJ, Mercer JF, McKeage MJ, 2010. Differential expression of ATP7A, ATP7B and CTR1 in adult rat dorsal root ganglion tissue. Mol Pain 6:53. [PubMed: 20836889]

Joe P, Getz M, Redman S, Petrilli M, Kranz TM, Ahmad S, Malaspina D, 2018. Serum zinc levels in acute psychiatric patients: A case series. Psychiatry Res. 261:344–50. [PubMed: 29334659]

Kardos J, Kovács I, Hajós F, Kálmán M, Simonyi M, 1989. Nerve endings from rat brain tissue release copper upon depolarization. A possible role in regulating neuronal excitability. Neurosci Lett. 103(2):139–44. [PubMed: 2549468]

Leary SC, Cobine PA, Kaufman BA, Guercin GH, Mattman A, Palaty J, Lockitch G, Winge DR, Rustin P, Horvath R, Shoubridge EA, 2007. The human cytochrome c oxidase assembly factors SCO1 and SCO2 have regulatory roles in the maintenance of cellular copper homeostasis. Cell Metab. 5(1):9–20. [PubMed: 17189203]

Lee J, Prohaska JR, Thiele DJ, 2001. Essential role for mammalian copper transporter Ctr1 in copper homeostasis and embryonic development. Proc Natl Acad Sci USA. 98(12):6842–7. [PubMed: 11391005]

Lim KO, Hedehus M, Moseley M, de Crespigny A, Sullivan EV, Pfefferbaum A, 1999. Compromised white matter tract integrity in schizophrenia inferred from diffusion tensor imaging. Arch Gen Psychiatry 56(4):367–74. [PubMed: 10197834]

Liu XH, Kato H, Nakata N, Kogure K, Kato K, 1993. An immunohistochemical study of copper/zinc superoxide dismutase and manganese superoxide dismutase in rat hippocampus after transient cerebral ischemia. Brain Res. 625(1):29–37. [PubMed: 7694776]

Mabry SJ, McCollum LA, Farmer CB, Bloom ES, Roberts RC, 2019. Evidence for altered excitatory and inhibitory tone in the post-mortem substantia nigra in schizophrenia. World Journal of Biological Psychiatry, 2019 6 4:1–18.

Marchetti C, 2014. Interaction of metal ions with neurotransmitter receptors and potential role in neurodiseases. Biometals 27(6):1097–113. [PubMed: 25224737]

Marshall CR, Howrigan DP, Merico D, et al., 2017. Contribution of copy number variants to schizophrenia from a genome-wide study of 41,321 subjects. Nat Genet. 49(1):27–35. [PubMed: 27869829]

Maryon EB, Molloy SA, Kaplan JH, 2013. Cellular glutathione plays a key role in copper uptake mediated by human copper transporter 1. Am J Physiol Cell Physiol. 304: C768–779. [PubMed: 23426973]

Matsushima GK, Morell P, 2001. The neurotoxicant, cuprizone, as a model to study demyelination and remyelination in the central nervous system. Brain Pathol. 11:107–116. [PubMed: 11145196]

Menkes JH, Alter M, Steigleder GK, Weakley DR, Sung JH, 1962. A sex-linked recessibe disorder with retardation of growth, pecular hair, and focal cerebral and cerebellar degeneration. Pediatrics 29:764–79. [PubMed: 14472668]

McCollum LA, McCullumsmith RE, Roberts RC, 2016. Tyrosine hydroxylase localization in the nucleus accumbens in schizophrenia. Brain Structure and Function. 221(9):4451–4458. [PubMed: 26740229]

McCullumsmith RE, Hammond JH, Shan D, Meador-Woodruff JH, 2014. Postmortem brain: an underutilized substrate for studying severe mental illness. Neuropsychopharmacology 39(1):65–87. [PubMed: 24091486]

Mohedano-Moriano A, Pro-Sistiaga P, Arroyo-Jimenez MM, Artacho-Perula E, Insausti AM, Marcos P, Cebada-Sanchez S, Martinez-Ruiz J, Munoz M, Blaizot X, Martinez-Marcos A, Amaral DG, Insausti R, 2007. Topographical and laminar distribution of cortical input to the monkey entorhinal cortex. J Anat. 211(2):250–60. [PubMed: 17573826]

Morrell A, Tallino S, Yu L, Burkhead JL, 2017. The role of insufficient copper in lipid synthesis and fatty-liver disease. IUBMB Life. 69(4):263–270. [PubMed: 28271632]

Mullin AP, Sadanandappa MK, Ma W, Dickman DK, VijayRaghavan K, Ramaswami M, Sanyal S, Faundez V, 2015. Gene dosage in the dysbindin schizophrenia susceptibility network differentially affect synaptic function and plasticity. J. Neurosci. 35, 325–338. [PubMed: 25568125]

Mutsuddi M, Morris DW, Waggoner SG, Daly MJ, Scolnick EM, Sklar P, 2006. Analysis of high-resolution HapMap of DTNBP1 (Dysbindin) suggests no consistency between reported common variant associations and schizophrenia. Am J Hum Genet. 79(5):903–9. [PubMed: 17033966]

Nazarian R, Starcevic M, Spencer MJ, Dell'Angelica EC, 2006. Reinvestigation of the dysbindin subunit of BLOC-1 (biogenesis of lysosome-related organelles complex-1) as a dystrobrevin-binding protein. Biochem J. 395(Pt 3): 587–598. [PubMed: 16448387]

Nickl-Jockschat T, Stöcker T, Markov V, et al., 2012. The impact of a Dysbindin schizophrenia susceptibility variant on fiber tract integrity in healthy individuals: a TBSS-based diffusion tensor imaging study. Neuroimage 60: 847–853. [PubMed: 22019876]

Norton N, Williams HJ, Owen MJ, 2006. An update on the genetics of schizophrenia. Curr Opin Psychiatry 19(2):158–64. Review [PubMed: 16612196]

Nguyen C, Schoonover KE, Mabry SJ, Farmer CB, Roberts RC, 2017. Characterization of copper transporter CTR1 in normal postmortem hippocampus. Society for Neuroscience, Washington DC.

Numakawa T, Yagasaki Y, Ishimoto T, et al. 2004. Evidence of novel neuronal functions of dysbindin, a susceptibility gene for schizophrenia. Hum Mol Genet. 13(21):2699–708. [PubMed: 15345706]

Pae CU, Drago A, Kim JJ, Patkar AA, Jun TY, Lee C, Mandelli L, De Ronchi D, Paik IH, Serretti A, 2008. DTNBP1 haplotype influences baseline assessment scores of schizophrenic inpatients. Neurosci Lett. 440(2):150–4. [PubMed: 18562100]

Papaleo F, Burdick MC, Callicott JH, Weinberger DR, 2014. Epistatic interaction between COMT and DTNBP1 modulates prefrontal function in mice and in humans. Mol Psychiatry 19(3):311–6. [PubMed: 24145376]

Perrin L, Roudeau S, Carmona A, Domart F, Petersen JD, Bohic S, Yang Y, Cloetens P, Ortega R, 2017. Zinc and Copper Effects on Stability of Tubulin and Actin Networks in Dendrites and Spines of Hippocampal Neurons. ACS Chem Neurosci. 8(7):1490–9. [PubMed: 28323401]

Petris MJ, Mercer JF, Culvenor JG, Lockhart P, Gleeson PA, Camakaris J, 1996. Ligand-regulated transport of the Menkes copper P-type ATPase efflux pump from the Golgi apparatus to the plasma membrane: a novel mechanism of regulated trafficking. EMBO J. 15(22):6084–95. [PubMed: 8947031]

Riley B, Kuo P-H, Maher BS, Fanous AH, Sun J, Wormley B, O'Neill FA, Walsh D, Zhao Z, Kendler KS, 2009. The dystrobrevin binding protein 1 (DTNBP1) gene is associated with schizophrenia in the Irish Case Control Study of Schizophrenia (ICCSS) sample. Schizophr Res. 115(2–3): 245–253. [PubMed: 19800201]

Roberts RC, Schoonover KE, Farmer CB, Morgan C, Sinha V, Odom L, 2019. Abnormal copper transporter CTR1 in postmortem schizophrenia hippocampus: a subregion and laminar analysis. Society for Neuroscience, 10 2019, Chicago, IL.

Roussos P, Katsel P, Davis KL, Siever LJ, Haroutunian V, 2012. A system-level transcriptomic analysis of schizophrenia using postmortem brain tissue samples. Arch Gen Psychiatry. 69(12):1205–1213. [PubMed: 22868662]

Samartzis L, Dima D, Fusar-Poli P, Kyriakopoulos M, 2014. White matter alterations in early stages of schizophrenia: a systematic review of diffusion tensor imaging studies. J Neuroimaging 24, 101–10. [PubMed: 23317110]

Sato M, Ohtomo K, Daimon T, Sugiyama T, Iijima K, 1994. Localization of copper to afferent terminals in rat locus ceruleus, in contrast to mitochondrial copper in cerebellum. J Histochem Cytochem. 42(12):1585–91. [PubMed: 7983358]

Scheggia D, Mastrogiacomo R, Mereu M, Sannino S, Straub RE, Armando M, Manago F, Guadagna S, Piras F, Zhang F, Kleinman JE, Hyde TM, Kaalund SS, Pontillo M, Orso G, Caltagirone C, Borrelli E, De Luca MA, Vicari S, Weinberger DR, Spalletta G, Papaleo F, 2018. Publisher Correction: Variations in Dysbindin-1 are associated with cognitive response to antipsychotic drug treatment. Nat Commun. 9(1):3560. [PubMed: 30158661]

Scheiber IF, Mercer JF, Dringen R, 2010. Copper accumulation by cultured astrocytes. Neurochem Int. 56(3):451–60. [PubMed: 20004225]

Schizophrenia Working Group of the Psychiatric Genomics, 2014. Biological insights from 108 schizophrenia-associated genetic loci. Nature 511(7510):421–7. [PubMed: 25056061]

Schoonover KE, Farmer CB, Cash AE, Roberts RC, 2019. Pathology of white matter integrity in three major white matter fasciculi: A post-mortem study of schizophrenia and treatment status. Br J Pharmacol.176(8):1143–55. [PubMed: 30735241]

Schoonover KE, Queern SL, Lapi SE, Roberts RC, 2018. Impaired copper transport in schizophrenia results in a copper-deficient brain state: a new side to the dysbindin story. World J Biol Psychiatry 1–17. [PubMed: 29345544]

Seitz J, Zuo JX, Lyall AE, Makris N, Kikinis Z, Bouix S, Pasternak O, Fredman E, Duskin J, Goldstein JM, Petryshen TL, Mesholam-Gately RI, Wojcik J, McCarley RW, Seidman LJ, Shenton ME, Koerte IK, Kubicki M, 2016. Tractography analysis of 5 white matter bundles and their clinical and cognitive correlates in early-course schizophrenia. Schizophr Bull. 42, 762–71. [PubMed: 27009248]

Sigmundsson T, Suckling J, Maier M, Williams S, Bullmore E, Greenwood K, Fukuda R, Ron M, Toone B, 2001. Structural abnormalities in frontal, temporal, and limbic regions and interconnecting white matter tracts in schizophrenic patients with prominent negative symptoms. Am J Psychiatry 158(2):234–43. [PubMed: 11156806]

Stan AD, Ghose S, Gao XM, Roberts RC, Lewis-Amezcua K, Hatanpaa KJ, Tamminga CA, 2006. Human postmortem tissue: what quality markers matter? Brain Res.1123(1):1–11. [PubMed: 17045977]

Stan AD, Ghose S, Zhao C, Hulsey K, Mihalakos P, Yanagi M, Morris SU, Bartko JJ, Choi C, Tamminga CA, 2015. Magnetic resonance spectroscopy and tissue protein concentrations together suggest lower glutamate signaling in dentate gyrus in schizophrenia. Mol Psychiatry 20(4):433–9. [PubMed: 24912493]

Straub RE, Jiang Y, MacLean CJ, Ma Y, Webb BT, Myakishev MV, Harris-Kerr C, Wormley B, Sadek H, Kadambi B, Cesare AJ, Gibberman A, Wang X, O'Neill FA, Walsh D, Kendler KS, 2002. Genetic variation in the 6p22.3 gene DTNBP1, the human ortholog of the mouse dysbindin gene, is associated with schizophrenia. Am J Hum Genet. 71(2):337–48. [PubMed: 12098102]

Talbot K, 2009. The sandy (sdy) mouse: a dysbindin-1 mutant relevant to schizophrenia research. In: Prog Brain Res, pp. 87–94, Elsevier.

Talbot K, Eidem WL, Tinsley CL, Benson MA, Thompson EW, Smith RJ, Hahn CG, Siegel SJ, Trojanowski JQ, Gur RE, Blake DJ, Arnold SE, 2004. Dysbindin-1 is reduced in intrinsic, glutamatergic terminals of the hippocampal formation in schizophrenia. J Clin Invest. 113(9):1353–63. [PubMed: 15124027]

Talbot K, Louneva N, Cohen JW, Kazi H, Blake DJ, Arnold SE, 2011. Synaptic dysbindin-1 reductions in schizophrenia occur in an isoform-specific manner indicating their subsynaptic location. PLoS One 6(3):e16886. [PubMed: 21390302]

Talbot K, Ong WY, Blake DJ, Tang J, Louneva N, Carlson GC, Arnold SE, 2009. Dysbindin-1 and Its Protein Family. In: Handbook of Neurochemistry and Molecular Neurobiology, pp. 107–241, Springer US.

Tang J, LeGros RP, Louneva N, Yeh L, Cohen JW, Hahn CG, Blake DJ, Arnold SE, Talbot K, 2009. Dysbindin-1 in dorsolateral prefrontal cortex of schizophrenia cases is reduced in an isoform-specific manner unrelated to dysbindin-1 mRNA expression. Hum Mol Genet. 18(20):3851–63. [PubMed: 19617633]

Tognin S, Viding E, McCrory EJ, et al., 2011. Effects of DTNBP1 genotype on brain development in children. J Child Psychol Psychiatry 52:1287–1294. [PubMed: 21639861]

Uranova NA, Vostrikov VM, Vikhreva OV, Zimina IS, Kolomeets NS, Orlovskaya DD, 2007. The role of oligodendrocyte pathology in schizophrenia. Int J Neuropsycho- pharmacology 10(4):537–45.

Varela-Gomez N, Mata I, Perez-Iglesias R, Rodriguez-Sanchez JM, Ayesa R, Fatjo-Vilas M, Crespo-Facorro B, 2015. Dysbindin gene variability is associated with cognitive abnormalities in first-episode non-affective psychosis. Cogn Neuropsychiatry 20(2):144–56. [PubMed: 25530342]

Vidovic B, Dordevic B, Milovanovic S, Skrivanj S, Pavlovic Z, Stefanovic A, Kotur-Stevuljevic J, 2013. Selenium, zinc, and copper plasma levels in patients with schizophrenia: relationship with metabolic risk factors. Biol Trace Elem Res. 156(1–3):22–8. [PubMed: 24150923]

Voisey J, Swagell CD, Hughes IP, Lawford BR, Young RM, Morris CP, 2010. Analysis of HapMap tag-SNPs in dysbindin (DTNBP1) reveals evidence of consistent association with schizophrenia. Eur Psychiatry 25(6):314–9. [PubMed: 20615671]

Vostrikov V, Orlovskaya D, Uranova N, 2008. Deficit of pericapillary oligodendrocytes in the prefrontal cortex in schizophrenia. World J Biol Psychiatry 9(1):34–42. [PubMed: 17853252]

Weickert CS, Rothmond DA, Hyde TM, Kleinman JE, Straub RE, 2008. Reduced DTNBP1 (dysbindin-1) mRNA in the hippocampal formation of schizophrenia patients. Schizophr Res. 98(1–3):105–10. [PubMed: 17961984]

Weickert CS, Straub RE, McClintock BW, Matsumoto M, Hashimoto R, Hyde TM, Herman MM, Weinberger DR, Kleinman JE, 2004. Human dysbindin (DTNBP1) gene expression in normal brain and in schizophrenic prefrontal cortex and midbrain. Arch Gen Psychiatry 61(6):544–55. [PubMed: 15184234]

Wilson SA, 1934. Kayser-Fleischer ring in cornea in two cases of Wilson's disease (Progressive Lenticular Degeneration). Proc R Soc Med. 27(3):297–8. [PubMed: 19989647]

Wolf C, Jackson MC, Kissling C, Thome J, Linden DE, 2011. Dysbindin-1 genotype effects on emotional working memory. Mol Psychiatry 16(2):145–55. [PubMed: 20010894]

Xuan Y, Yan G, Wu R, Huang Q, Li X, Xu H, 2015. The cuprizone-induced changes in (1)H-MRS metabolites and oxidative parameters in C57BL/6 mouse brain: Effects of quetiapine. Neurochem Int. 90:185–92. [PubMed: 26340869]

Yamaguchi Y, Heiny ME, Suzuki M,. Gitlin JD, 1996. Biochemical characterization and intracellular localization of the Menkes disease protein. Proc Natl Acad Sci USA. 93(24):14030–5. [PubMed: 8943055]

Zatz M, Vallada H, Melo MS, Passos-Bueno MR, Vieira AH, Vainzof M, Gill M, Gentil V, 1993. Cosegregation of schizophrenia with Becker muscular dystrophy: susceptibility locus for schizophrenia at Xp21 or an effect of the dystrophin gene in the brain? J Med Genet. 30(2):131–4. [PubMed: 8445617]

Zhang Y, Xu H, Jiang W, Xiao L, Yan B, He J, Wang Y, Bi X, Li X, Kong J, Li XM, 2008. Quetiapine alleviates the cuprizone-induced white matter pathology in the brain of C57BL/6 mouse. Schizophr Res.106(2–3):182–91. [PubMed: 18938062]

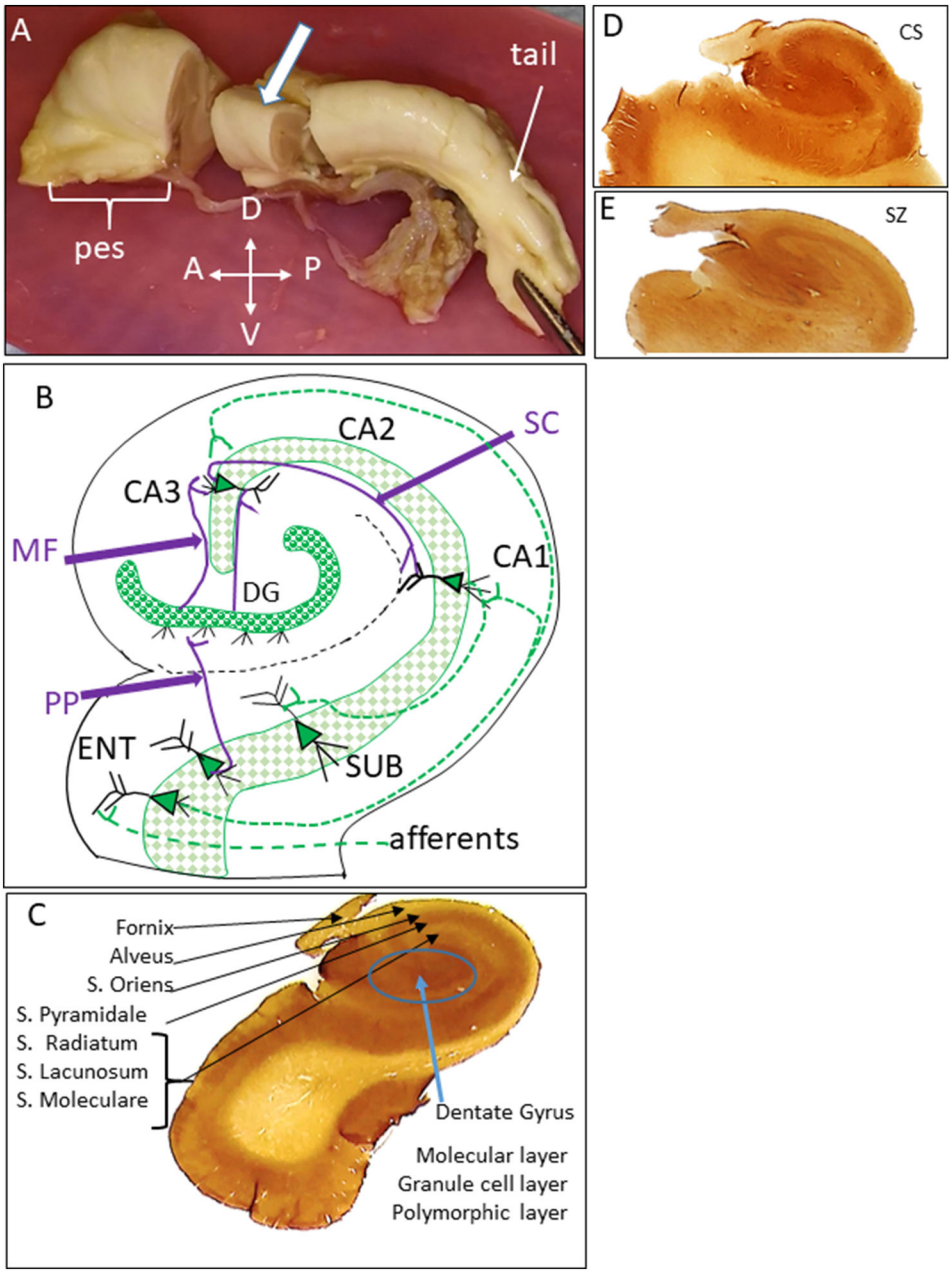

Figure 1.

A) Whole hippocampus from a comparison subject (C3) with the anterior portion of the body subdissected prior to being cut in coronal sections on the vibratome. The pes and the tail of the hippocampus are indicated. Directional coordinates are included. B) A simplified diagram of the hippocampal formation with the various regions labeled. The connections of the hippocampal trisynaptic pathway are indicated in purple: axons of the perforant path (PP), mossy fibers (MF) and Schaffer collaterals (SC) are purple. Other connections are indicated by dashed green lines representing axons. Dendrites are black. The granule cell layer of the dentate gyrus is outlined and filled with green spheres indicating excitatory granule cells. The pyramidal cell layer is outlined and filled with green diamond shapes

indicating excitatory pyramidal neurons. The dotted black line indicates the hippocampal fissure. C) The layers of the hippocampus proper and dentate gyrus (DG) identified in a dysbindin immunolabeled section. Section is from a comparison subject (C10). D,E) Hippocampus proper and dentate gyrus immunolabeled for CTR1 in a comparison subject (CS, C5) and schizophrenia patient (SZ, S10). S, stratum. ENT, entorhinal cortex. DG, dentate gyrus. SUB, subiculum.

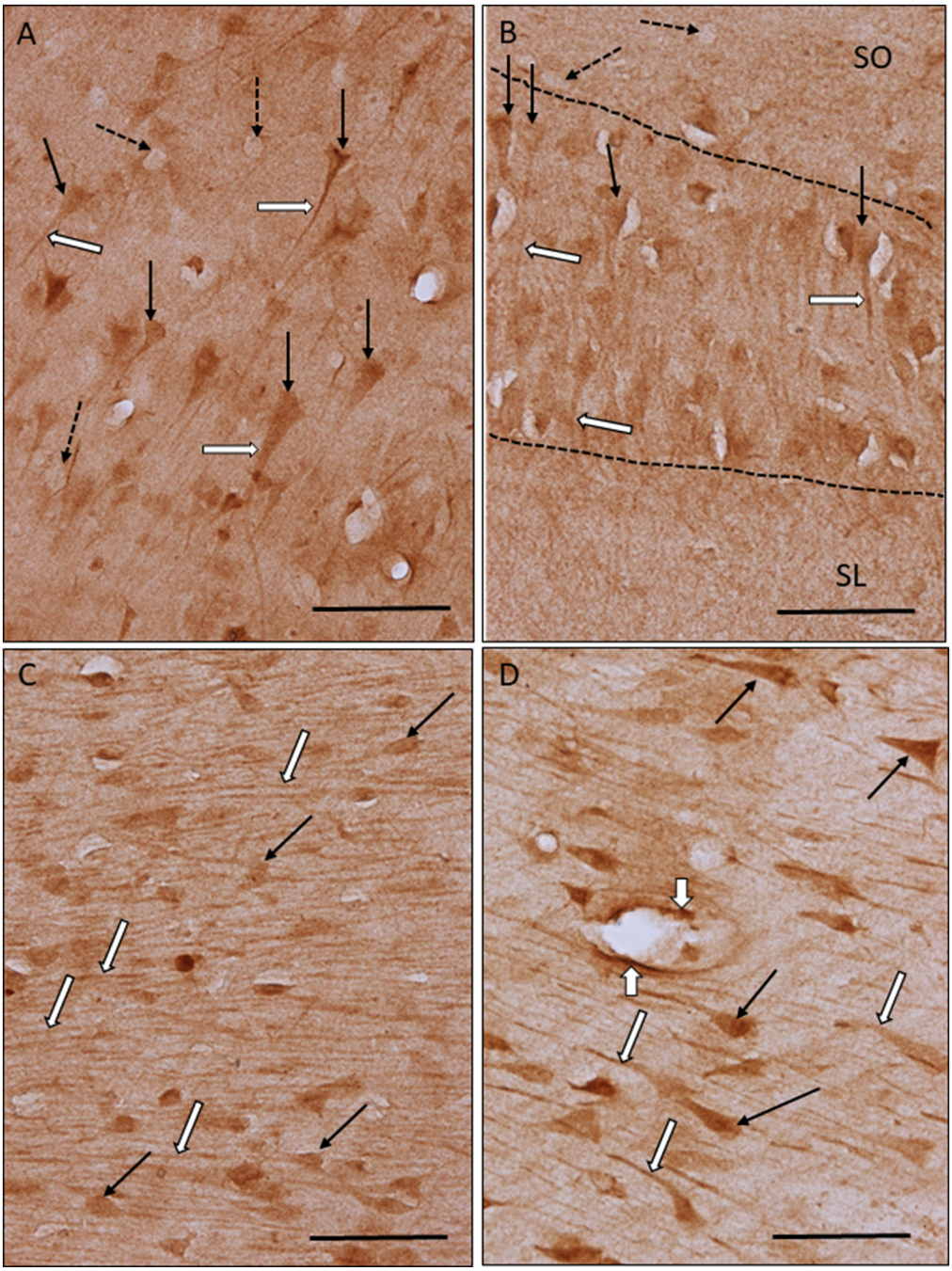

Figure 2.

CTR1- immunolabeled pyramidal layers with examples of immunolabeled pyramidal neurons (black arrows), their apical dendrites (black and white arrows) and unlabeled cells (dashed arrows). A) Entorhinal cortex from C10. B) CA3 showing stratum oriens (SO), the pyramidal layer (outlined by dotted lines) and stratum lacunosum (SL) from C5. C) CA1 pyramidal layer from C3. The pyramidal cell layer in CA1 is larger than that of CA3; thus the pyramidal cell layer occupies this entire micrograph. D) The subiculum from C3.

Labeled endothelial processes are indicated by white arrows lined in black. Scale bars = 100μm.

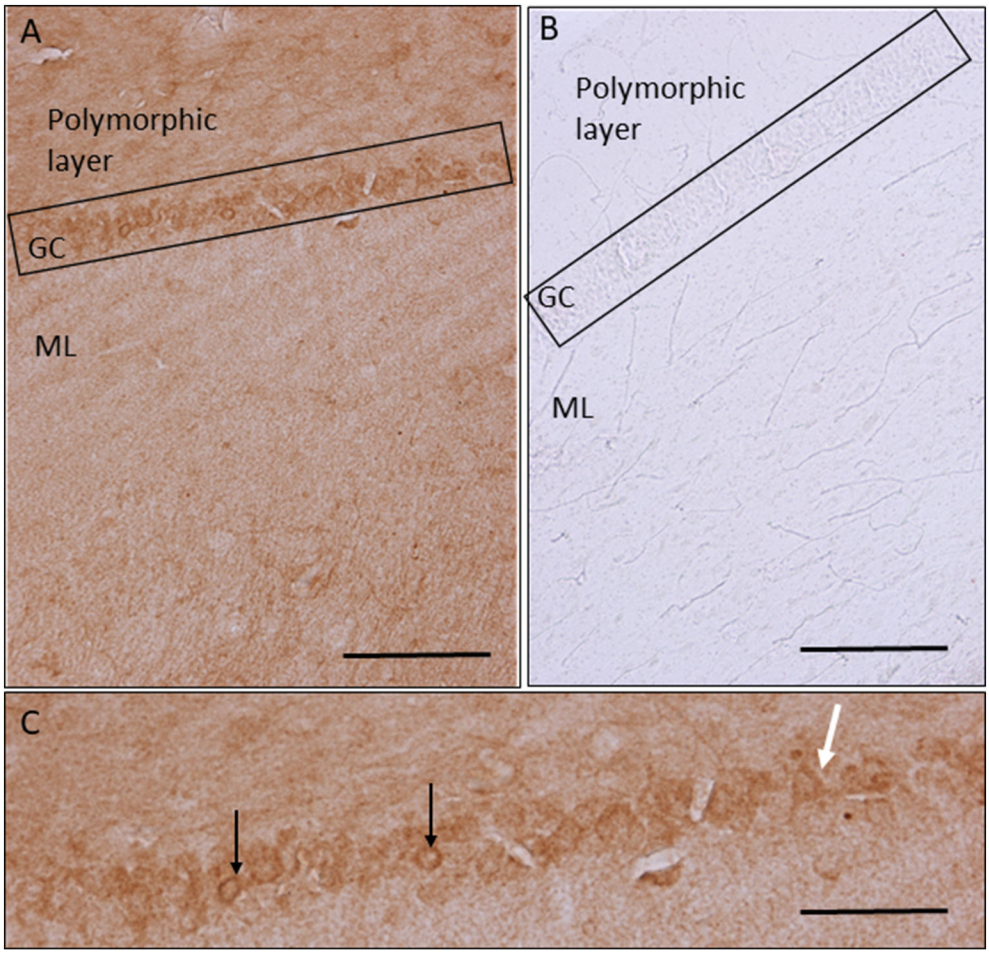

Figure 3.

A) CTR1-immunolabeled layers of the dentate gyrus from C5. B) Antibody control in C3 consisting of omitting the primary antibody; no labeling is present. C) Higher magnification micrograph of the boxed area in A. Solid black arrows point to immunolabeled granule cells in the granule cell layer (GC) of the dentate gyrus. Solid white arrow points to an immunolabeled interneuron ML, molecular layer. Scale bars = 100μm (A,B), 50 μm (C).

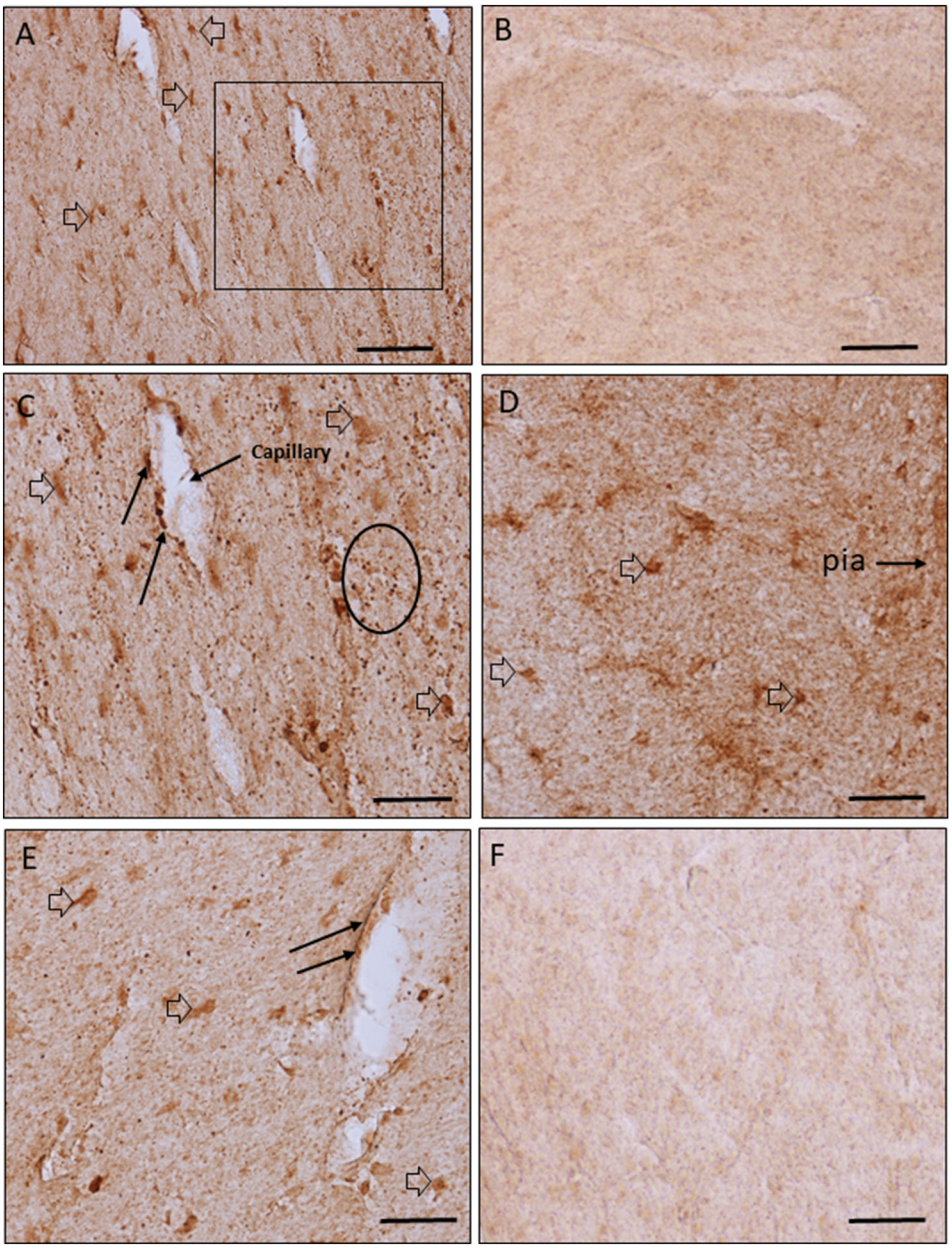

Figure 4.

A) CTR1- immunolabeled section from the fornix of case C5. Immunolabeled glial cells are indicted (open arrows). The boxed area is shown at higher magnification in C. B) Preadsorption control in the fornix from C3 results in no specific immunolabeling. C) Enlargement of boxed area in A. Labelled endothelial cells (arrows) partially surround a capillary; immunolabeled glial cells are indicted (open arrows). Examples of labeled punctate structures (in circle) that are especially prominent in the fornix. D) The alveus contains immunolabeled glial cells (open arrows). The direction of the pia mater is indicated with a solid arrow. E) Subcortical white matter in the subiculum. Open arrows indicate immunolabeled glial cells. Black arrows indicate immunolabeled endothelial cells. F)

Preadsorption control in the subcortical white matter in the subiculum in C3 results in no specific immunolabeling.
Scale bars = A,B, D-F) 100μm, C) 50μm.

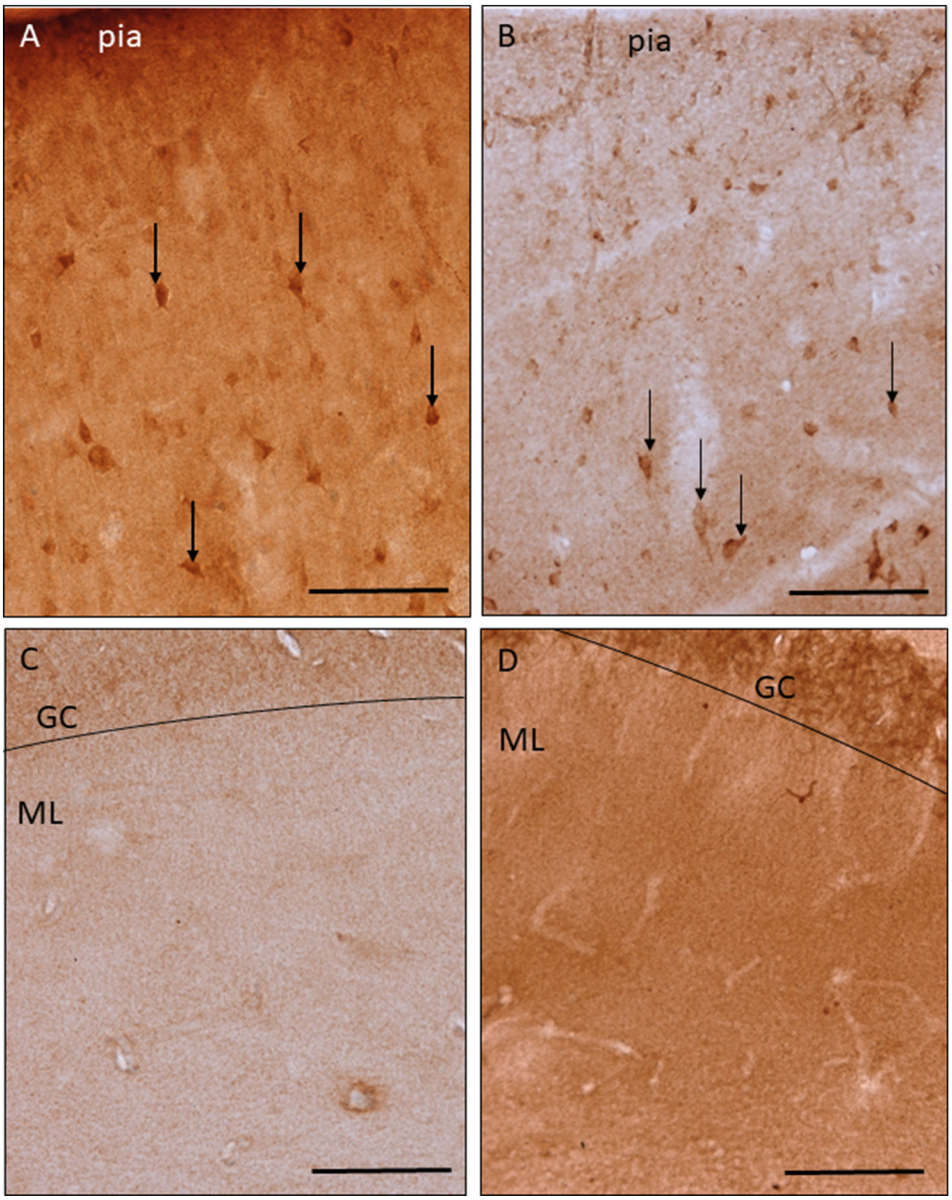

Figure 5.

CTR1 immunolabeling in the entorhinal cortex and dentate gyrus where significant differences were found between groups. These photomicrographs illustrate extreme differences between comparison subjects and patients with schizophrenia. A, B) CTR1 immunolabeling in the superficial layers of the entorhinal cortex in a comparison subject (C1) and a patient with schizophrenia (S3), respectively. Immunolabeling was denser in the comparison subject than in the schizophrenia patient. Arrows indicate immunolabeled neurons. C, D) CTR1 immunolabeling in the granule cell (GC) and molecular layer (ML) of the dentate gyrus in a comparison subject (C5) and a patient with schizophrenia (S8), respectively. Immunolabeling was lighter in the comparison subject than in the schizophrenia patient. Scale bars = 100μm.

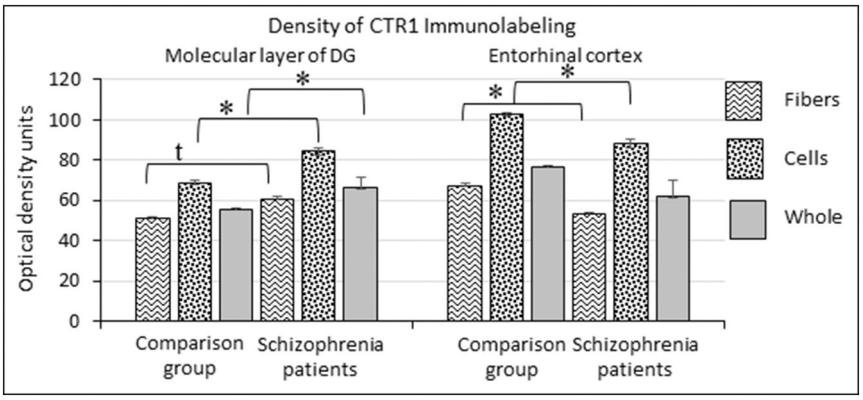

Figure 6.

Graph shows differences in optical density (OD) units in the dentate gyrus (DG) and entorhinal cortex between groups. Both cells and the whole image of the molecular layer had significantly higher OD values in schizophrenia patients than comparison subjects. In the superficial areas of the entorhinal cortex, both fibers (neuropil) and cells showed less OD values in the schizophrenia patients than in comparison subjects. Error bars depict the standard error of the mean. Asterisks denote significance ($p<0.05$); “t” denotes a trend $0.1>p>0.05$.

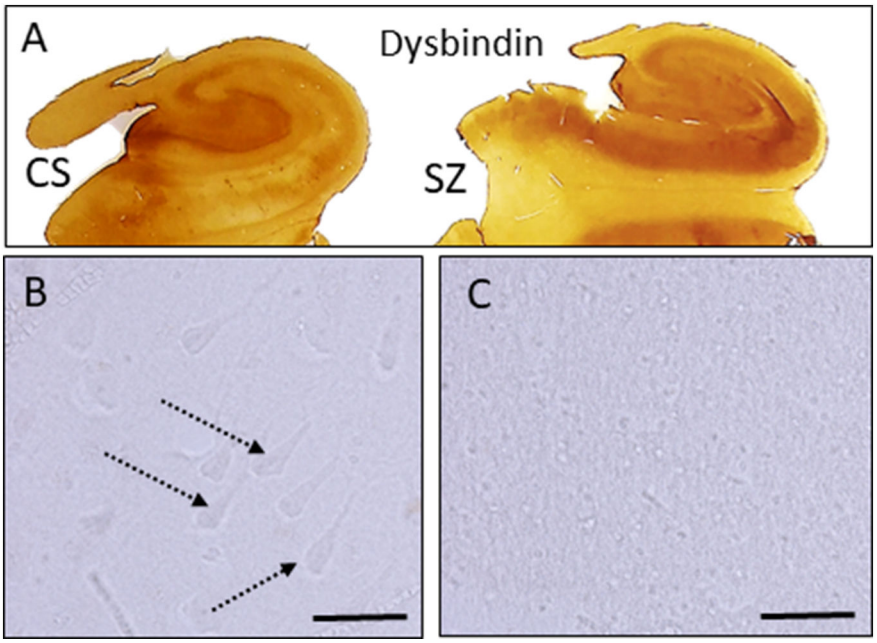

Figure 7.

A) Dysbindin immunolabeled sections of the hippocampus in a comparison subject (C5) and a patient with schizophrenia (S10). The density and distribution of dysbindin immunolabeling was similar between groups. B, C) Dysbindin controls showing complete lack of immunostaining after omitting the primary antibody in CA1 pyramidal layer (B) and entorhinal cortex of case C3 (C). Scale bars = 50μm.

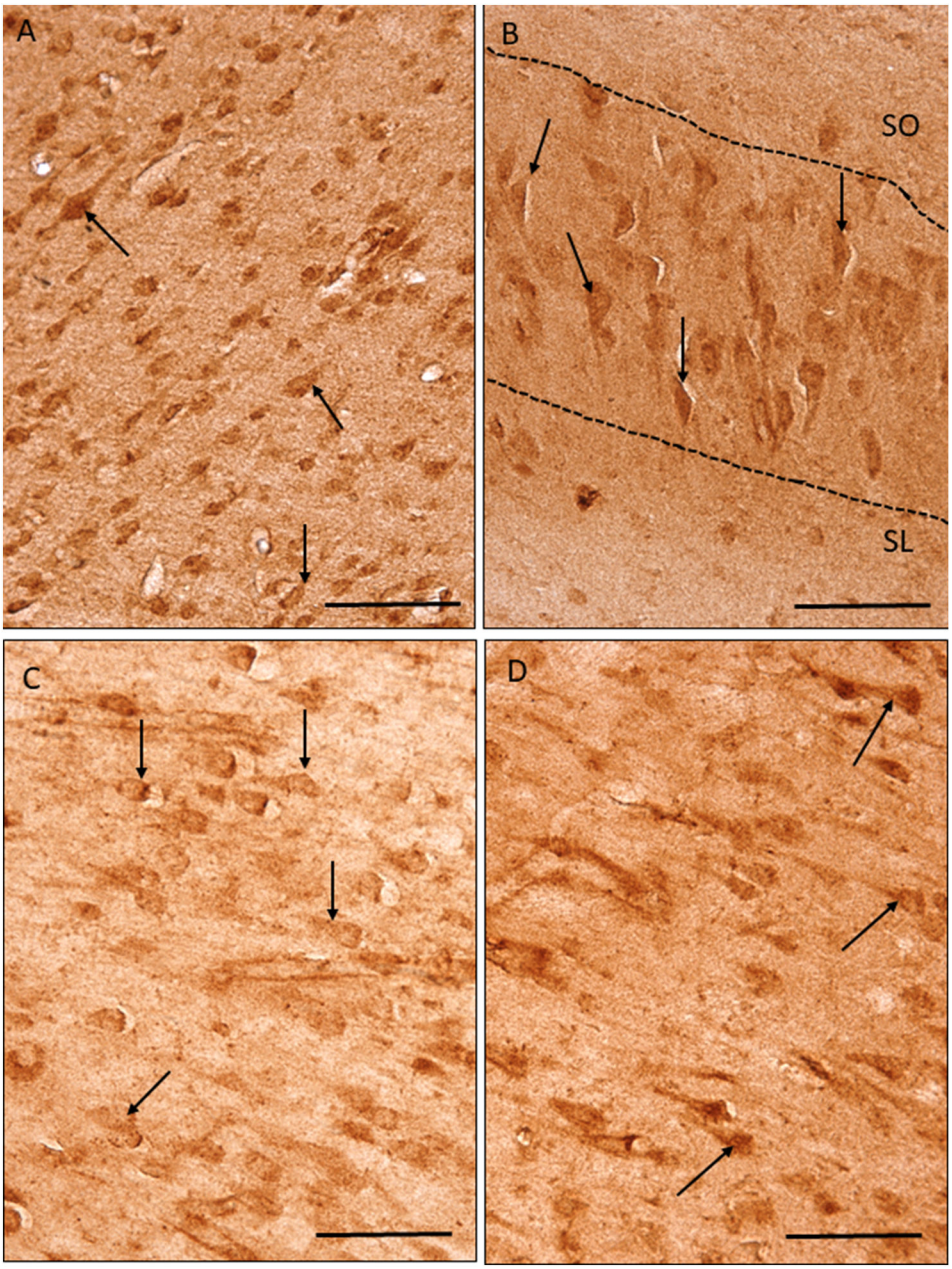

Figure 8.

A) Dysbindin immunolabeled pyramidal layers with examples of immunolabeled pyramidal neurons (black arrows) from C5. A) Entorhinal cortex. B) CA3 showing stratum oriens (SO), the pyramidal layer (outlined by dotted lines) and stratum lacunosum(SL) from C5. C) CA1 pyramidal layer. D) The subiculum. Scale bars = 100μm.

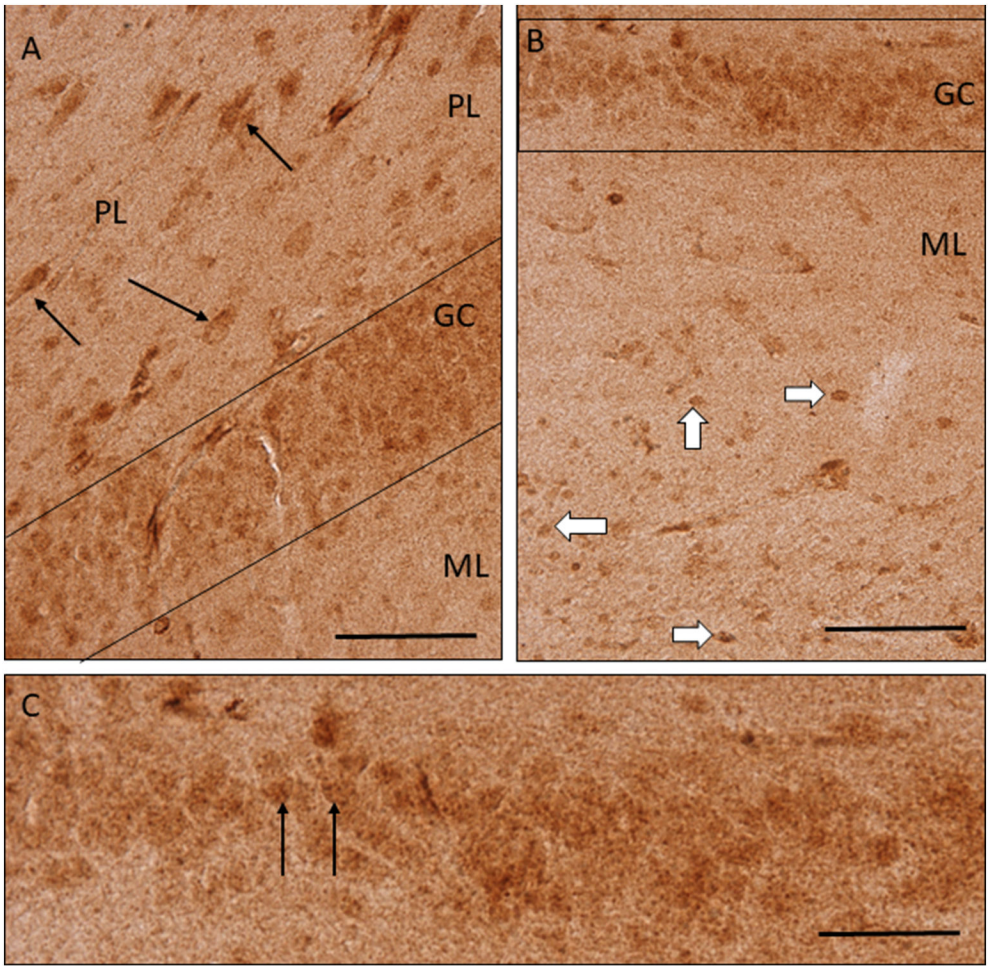

Figure 9.

A) Dysbindin immunolabeling of the dentate gyrus from C5. Neurons are immunolabeled in the polymorphic layer (PL) with arrows. Dense immunolabeling is present in the granule cell (GC) layer. B) Another view of the dentate gyrus showing the GC layer and the molecular layer (ML). Black and white arrows indicate immunolabeled glial cell in the ML. C) Higher magnification micrograph of the boxed area in B. Solid black lines point to granule cells that may be immunolabeled. The density of the labeling in the GC layer makes it difficult to distinguish labeling in soma from labeling in the neuropil. Scale bars = 100μm (A,B), 50 μm (C).

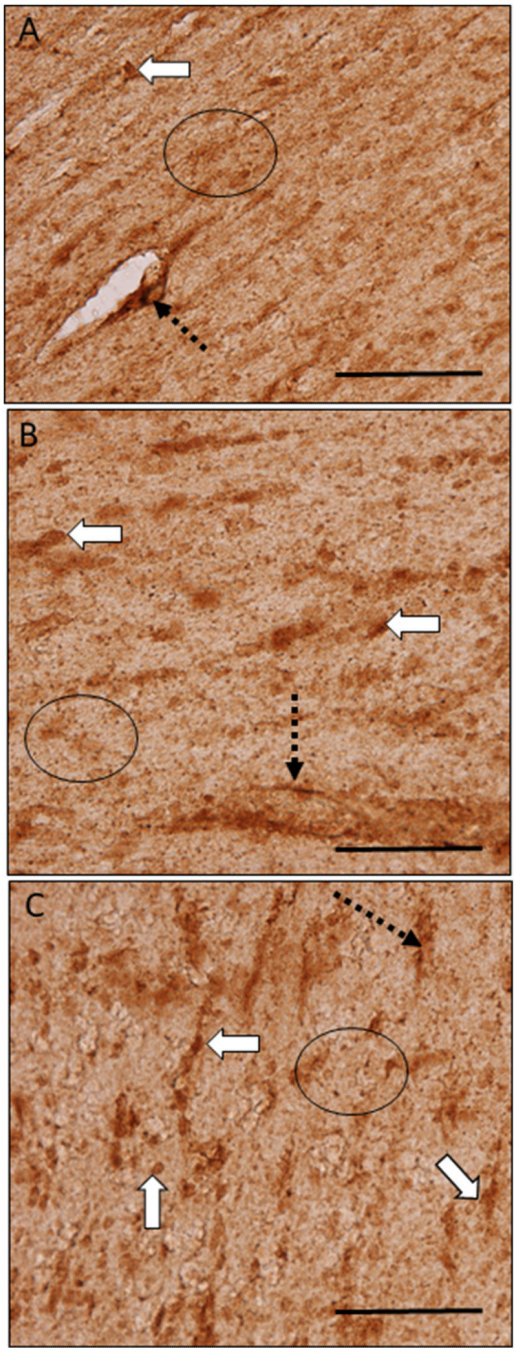

Figure 10.

Dysbindin immunolabeling in white matter of case C5. A) Fornix. B) The alveus over CA3. C) Subcortical white matter in the subiculum. Immunolabeled glial cells are indicated by black and white arrows. Labelled endothelial cells (dotted arrows) partially surround capillaries. Examples of labeled punctate structures (in circles). Scale bars = 100μm.

Table 1.

Individual demographics for subjects in the comparison group (CG) and the patients with schizophrenia (SZ).

CG	Age years	sex	race	PMI	pH	Cause of death	APD	TIF CTR1	TIF Dys
1	86	M	AA	6	7.32	Gun shot wound	NA	240	243
2	43	F	C	8	6.66	Alcoholism	NA	144	147
3	40	M	AA	7	6.68	Cardiac arrhythmia	NA	137	140
4	42	M	H	8	6.25	cancer	NA	157	160
5	35	M	C	4	6.70	Motor vehicle accident	NA	266	269
6	43	F	AA	6	6.92	pneumonia	NA	158	161
7	37	F	C	5	7.03	ASCVD	NA	235	238
8	32	F	C	8	6.30	Cardiac arrest	NA	93	96
9	32	F	C	7	7.37	Cardiac arrhythmia	NA	243	246
10	45	F	AA	8	6.93	cardiomegaly	NA	179	182
Mean ± SD	43.5±15.6	4M 6F	4AA 5C 1H	6.7±1.42	6.82±0.38			185.2±57.20	188.2±57.20
SZ									
1	78	M	C	6	6.47	pneumonia	unk	162	165
2	56	F	C	6	6.34	drug overdose	unk	154	157
3	45	M	C	6	7.17	Drug overdose	aAPD	204	207
4	47	M	C	8	6.98	ASCVD	RIS	235	238
5	43	M	AA	4	unk	seizure	THZ	229	232
6	59	F	AA	3	7.04	ASCVD	CLP	301	304
7	33	F	AA	3	6.83	drug overdose	off	232	235
8	60	F	AA	6	unk	DVT	LOX	198	201
9	52	F	C	5	7.05	Choked on food	RIS	237	240
10	60	M	AA	5	unk	amyloidosis	aAPD	205	208
Mean±SD	53.3±12.3	5M 5F	5AA 5C	5.2±1.55	6.84±0.32			215.7±41.89	218.7±41.89
P=	0.137			0.037	0.892			0.191	0.191
χ^2		0.653	0.574						

Subjects were not paired. ARS: age, race, sex. PMI, postmortem interval in hours. TIF, time in fixative in months. APD, antipsychotic drugs. NA, not applicable. AA, African-American. C, Caucasian. H, Hispanic. M, male. F, female. ASCVD, atherosclerotic cardiovascular disease. DVT, deep vein thrombosis. Unk, unknown. aAPT, atypical APD. CLP, chlorpromazine. THZ, Thioridazine. RIS, Risperidol. LOX, Loxapine. P values are given for unpaired t-tests.